SATELLITE TARGET SIGNATURE STUDY USING CLOSE RANGE MILLIMETER WAVE IMAGING TECHNIQUES

J. Mark Baird

Hughes Research Laboratories

Prepared for:

Advanced Research Projects Agency
Army Missile Command

December 1973

SATELLITE TARGET SIGNATURE STUDY USING CLOSE RANGE MILLIMETER WAVE IMAGING TECHNIQUES

MARK BAIRD

HUGHES RESEARCH LABORATORIES
3011 MALIBU CANYON ROAD
MALIBU, CA 90265

DECEMBER 1973

CONTRACT DAAHOI-73-C-0628
SEMIANNUAL TECHNICAL REPORT
1 APRIL 1973 through 31 OCTOBER 1973

ARPA ORDER 2320

Sponsored by
ADVANCED RESEARCH PROJECTS AGENCY
1400 WILSON BOULEVARD
ARLINGTON, VA 22209

Monitored by
U.S. ARMY MISSILE COMMAND
REDSTONE ARSENAL, AL 35809

UNCLASSIFIED

SECURITY CLASSIFICATION OF THIS PAGE (When Data Entered)

REPORT DOCUMENTATION PAGE		READ INSTRUCTIONS BEFORE COMPLETING FORM
1. REPORT NUMBER: Semiannual Tech. Rpt.	2. GOVT ACCESSION NO.	3. RECIPIENT'S CATALOG NUMBER
4. TITLE (and Subtitle): Satellite Target Signature Study Using Close Range Millimeter Wave Imaging		5. TYPE OF REPORT & PERIOD COVERED: Semiannual Tech. Rpt. 1 April 1973-31Oct1973 6. PERFORMING ORG. REPORT NUMBER
7. AUTHOR(s): J.M. Baird		8. CONTRACT OR GRANT NUMBER(s): DAAH01-73-C-0628
9. PERFORMING ORGANIZATION NAME AND ADDRESS: Hughes Research Laboratories, 3011 Malibu Canyon Road, Malibu, CA 90265		10. PROGRAM ELEMENT, PROJECT, TASK AREA & WORK UNIT NUMBERS
11. CONTROLLING OFFICE NAME AND ADDRESS: U.S. Army Missile Command, Redstone Arsenal, AL 35809		12. REPORT DATE: December 1973 13. NUMBER OF PAGES: 37
14. MONITORING AGENCY NAME & ADDRESS (if different from Controlling Office)		15. SECURITY CLASS. (of this report): Unclassified 15a. DECLASSIFICATION/DOWNGRADING SCHEDULE
16. DISTRIBUTION STATEMENT (of this Report)		
17. DISTRIBUTION STATEMENT (of the abstract entered in Block 20, if different from Report)		
18. SUPPLEMENTARY NOTES		
19. KEY WORDS (Continue on reverse side if necessary and identify by block number): Millimeter wave imaging Space object imaging		

20. ABSTRACT (Continue on reverse side if necessary and identify by block number)

An experimental design and test setup is described by which 94 GHz images of satellite type targets or portions thereof can be obtained at close range for the purpose of determining the effectiveness of millimeter wavelength range-doppler radar in space object imaging applications.

The close range imaging technique uses two parabolic antennas which are both focused at short range on the same

DD FORM 1 JAN 73 1473 EDITION OF 1 NOV 65 IS OBSOLETE

UNCLASSIFIED

SECURITY CLASSIFICATION OF THIS PAGE (When Data Entered)

target element. These antennas are then mechanically rotated together as a unit so that the rf spot in the target plane is raster scanned over the target. The received signal versus scan position is used to display the target image. First results are expected at the end of 1973.

TABLE OF CONTENTS

LIST OF ILLUSTRATIONS

I. INTRODUCTION

This report is the Semiannual Technical Report fulfilling ELIN A002 of Micom Contract DAAH01-73-C-0628 under the support of ARPA. The purpose of this program is to obtain millimeter wave images of satellite structures to determine the usefulness of a millimeter wave range-doppler radar for the characterization of space objects. In this report we describe how the program methodology has evolved and review the on-going program effort.

The original program plan involved the use of an existing image dissecting panel which would provide real time images. This device had been developed by Hughes for the USA ECOM, Fort Monmouth, and used a 20 x 20 element array of PIN diodes capable of being electronically scanned at a 30 frames/sec rate. The normal state of each PIN diode provided for direct charge injection so the element would absorb the incident millimeter wave energy which had been reflected from the target in question. During a raster scan, the injected current was reduced to zero in each diode in a time sequential fashion to provide a flying window in an otherwise opaque panel. Thus, it would be possible to provide, in a laboratory environment, a comprehensive study of target signatures of satellite structures at 94 GHz. The real-time performance of the system would provide a rapid complete pictorial record of images for many targets from all significant angles of view. Since interest was also expressed in determining the wavelength dependent differences in images of the same target, it was originally proposed to also make 35 GHz images of a few selected target views for comparison with the 94 GHz data. This was to be done by mechanically scanning a waveguide probe and detector in the image plane of a 35 GHz lens.

After the program was initiated and progressing along the lines described above, it became evident through on-going discussions with government representatives that the originally proposed program plan was not going to meet the needs of the government in two specific areas. First, the average dynamic range (on/off attenuation ratio) of each diode element in the image dissecting panel is about 22 dB. Thus,

the resultant image would have a relatively poor signal/noise ratio and, depending on the target detail, make it difficult to resolve small scattering centers. Second, the image dissecting panel method could not be duplicated at lower frequencies and thus the comparison with images at other frequencies would be open to question.

At a review meeting held in Washington during May 1973, the decision was made to abandon the use of the 94 GHz image dissecting panel in favor of a conventional angle-angle scan of a suitable target on a 50 ft outdoor range at both 94 and 6 GHz. This technique involves flooding the target with each rf frequency and scanning a focused receiver aperture over the target to provide an image. It should be pointed out that we were seeking more than just the normal radar cross section measurement of a target; actual images require both phase and amplitude information about the reflected rf energy. At this point alternate schemes were investigated, and these are discussed more fully in Section II with a discussion of advantages and disadvantages of each method. The techniques that did not require the use of an anechoic chamber were of greatest interest because such a facility was not available for this program.

The planned approach had the advantage of providing images at the two frequencies by exactly comparable techniques. Moreover, since a large body of range doppler images at 6 GHz existed, a comparison of these data with the angle-angle scan data at 6 GHz should lead to good estimates of the expected results from a 94 GHz range-doppler system based on the 94 GHz angle scan data. This comparison, of course, has been an objective of the signature program since its inception.

In August 1973, at a review meeting held at Culver City, California, the plans for the comparative 6 GHz data were dropped. It was also decided to use a focused transmitter source as well as a focused receiver aperture to improve the sidelobe problem inherent with any antenna range system. Work has been proceeding toward establishing an instrumented outdoor range at HRL in Malibu where the natural terrain feature should provide for low clutter returns from the nearby environment.

During the course of the program, an effort has been made to acquire suitable target structures for investigation. It was originally planned to use actual satellites as built and available from the Hughes Space and Communications Group in El Segundo, California. Such targets are available for use with the image dissecting panel equipment since this unit is small and mobile enough to be used at the facility where the actual satellites are being manufactured and tested. Such actual satellites are not available for use at an outdoor signature range at Malibu for obvious reasons of cost, risk, and flight schedules. Therefore, it was planned to use cannonical shapes, simulated satellite details, and perhaps some real solar panels of small size. Discussions with Lincoln Laboratories have indicated that we may be able to borrow the qualification model of the LES-6 satellite which is now surplus to their needs. This unit has simulated solar panels but has considerable other details of satellite construction which would be interesting to image and analyze at 94 GHz. In addition, a large body of backscatter data exists which was taken with this target at both X-band frequencies and at 10.6 μm. Thus it would provide an excellent comparison vehicle for data taken at three widely separated wavelengths.

It has been proposed to ARPA that the existing program be extended to allow for more image data to be gathered and analyzed than is possible within the scope of the original program and that additional targets include the existing LES-6 qualification model hardware. A program extension of six months was proposed for this added effort.

II. SURVEY OF MILLIMETER WAVE IMAGING TECHNIQUES

A. General Considerations

Since the purpose of this program is to determine the usefulness of a 3.2 mm range-doppler radar for imaging and identifying the geometric features of satellite targets, it would be ideal if the experiments performed could use the range-doppler radar imaging technique. This technique, however, involves rapid and accurately measured translational motion of either the target or the transceiver and is not within the scope of the present effort. Therefore, we have considered many alternative rf imaging techniques in terms of their ability to yield the desired information and their relative complexity. The results of this effort are described in this section.

The imaging techniques considered here tend to fall into two general categories which we have termed direct and indirect imaging. By direct imaging, we mean those experiments in which the image is obtained directly by mechanically scanning some part of the imaging system while sensing the return signal. The direct methods described only require an AM or an FM cw receiver and the image can be printed out during the scanning operation. This is contrasted with indirect imaging methods which require the measurement of both amplitude and phase (or doppler) during the mechanical scanning process and then subsequent data transformation via digital computer to obtain the image. Indirect methods thus require a receiver which is phased referenced to the rf transmitter (or capable of doppler discrimination), and the image is only obtained after the entire scan is completed and the data are processed as a whole. In general, the indirect imaging techniques require more sophisticated equipment to obtain the data and more elaborate data processing to get the final image, whereas direct imaging allows the results to be evaluated at the data are taken. Indirect imaging techniques will be considered first.

B. Indirect Imaging Techniques

Indirect imaging methods can be divided into two subcategories — those which resolve the target in range-angle (i.e., in a range-cross range plane) and those which resolve the target in angle-angle (the normal photographic sense of image plane resolution).

The best technique for obtaining range-angle resolution of a target (and the one which most closely simulates the range-doppler radar imaging technique) is to take phase and amplitude backscatter measurements using a coherent short pulse radar. The measurements are taken while the target is rotated through a desired angle of view and the data as a whole are then processed into an image which cuts through the target in the plane parallel to the range and transverse to the axis of rotation. This is the same view seen by a range-doppler radar on a satellite which is stable with respect to the surface of the earth. This technique requires the use of some very sophisticated equipment and experimental procedures to implement. The 94 GHz transmitted signal would have to be derived from a stable oscillator chopped into subnanosecond pulses and amplified by a broadband 94 GHz TWT power amplifier. The receiver must then be capable of resolving the time and phase relationships of the return pulses from the target. This wideband receiving equipment can be simplified by the use of a sampling oscilloscope. One major area of concern is the requirement for target stability during the measurement series. At these short wavelengths, 10° of phase change occurs with only 0.089 mm (0.0035 in.) of movement.

Two additional methods for indirect imaging which give range-angle type images are the doppler radar and the FM cw radar techniques. The doppler radar imaging technique is implemented by fixing the rf illuminating source and receiver at the desired range and spinning the target about a transverse axis at a sufficiently high rate of speed to obtain detectable doppler frequency shifts. By separating the return signals into doppler "bins" and recording the angular positions at which they occur, it is possible to process the data into a two-dimensional cross-sectional view of the target transverse to the axis of rotation.[1]

The FM cw radar imaging technique uses an FM cw radar with the desired range resolution to measure backscatter versus range while rotating the target through a complete revolution. As with the spinning target doppler method, it is possible to process the data into a two-dimensional cross-sectional view transverse to the axis of rotation.

These two techniques both require the use of less sophisticated equipment than the coherent pulse method since phase measurements are not required. A serious question arises, however, from the fact that millimeter wave scattering centers tend to be made up of relatively narrow angle glints, whereas the doppler and FM cw methods just described require that the scattering centers be "seen" through a major portion of a revolution. The effects on the images in this case have not been determined but the expected problems are deemed to be serious.

For angle-angle type indirect images it is immediately obvious that the elegant way to take phase and amplitude measurements over an aperture is to use an array antenna. For the current program, however, all methods involving arrays were excluded because of the time and expense involved in fabricating arrays. We limit the discussions here to the use of a single receiver with data taken by mechanically moving either the receiver or target. Two methods for obtaining phase and amplitude data that can be processed into images include:

1. Illuminate the target from a fixed rf source and mechanically position the receiver at discreet points in a receiving aperture while recording the amplitude and phase relative to the transmitted signal.

2. Fix the rf illuminating source and receiver and mechanically move or rotate the target to simulate all of the angles of view in the receiving aperture.

These two imaging methods still have the problem of maintaining the mechanical stability of the target and transceiver within a small portion of a wavelength. Overcoming this problem appears to be simply a matter of experimental sophistication. For example, at 3.2 mm, it would be required to take data over an aperture of about

20 in. diameter (for 14 m range) with position tolerance in the scanning plane maintained at about 0.005 in. This would require careful design.

One advantage of these two direct imaging methods is the fact that a cw coherent transceiver is much easier to implement than a coherent pulse transceiver. Also, in case No. 1 above, the image is obtained by simply taking the Fourier transform of the signal recorded in the aperture plane. Thus with the addition of real time A/D conversion and a fast Fourier transform minicomputer (both of which are readily obtainable), it would be possible to get near-real-time operation.

C. Direct Imaging Techniques

Because of the limited scope of the present program, direct imaging techniques have been given prime consideration for this project. These techniques not only require simpler transceivers, but since they do not require phase measurements, the mechanical stability of the target becomes far less critical and is essentially eliminated as a problem.

Once again it is possible to divide the direct imaging techniques into two categories: those which yield range-angle images and those which give angle-angle type images. Two variations of a technique which yields range-angle images and four techniques which give angle-angle images will be described here.

Direct images that resolve the target in range and angle can be produced by combining a range radar with two focused fan beam antennas. The range radar can take either of two forms: An FM cw radar or a subnanosecond pulse radar. Of the two, it would be easier at Hughes Research Laboratories to implement the FM cw radar technique since our existing backward wave oscillator (BWO) could be used as the swept frequency source. The angular (cross range) resolution of the target is obtained by using two fan beam antennas (transmitter and receiver) which are both focused on the same target element and scanned together as a unit. In operation the focused fan beams are scanned slowly across the target and the received signal is spectrum analyzed to determine the amplitude of the return signals from each range

resolution element within the target depth of range. These amplitudes are then displayed as functions of range and angle to give the desired image.

Although this FM cw radar with scanning fan beam antennas is easier to implement than a coherent pulse radar, it still represents a degree of complexity far greater than that required for simple angle-angle scanned images. The fan beam antennas would have to be specially designed, the transmitter would require a power supply modulator, and the receiver would have to include provision for spectrum analysis with the required degree of range resolution. The deterioration of range resolution with frequency sweep rate and nonlinearities needs to be investigated further and could be a source of difficulties in building the transceiver.

Four direct imaging techniques that can be used to obtain angle-angle type images at millimeter wave frequencies are listed below.

1. Flood the target with rf energy and image the return signals with a lens or focused reflector. The detector is scanned in the image plane or the reflector is angle scanned.

2. Scan the target with a resolution size rf beam while monitoring the return signal.

3. A combination of No. 1 and No. 2 wherein both the transmitter receiver antennas are focused on the same element in the target plane and scanned together as a unit.

4. Scan a resolution size hole in an absorptive panel in front of the target while flooding with rf and monitoring the return signal. (The target also may be scanned behind the hole.)

Of these four methods, the first and the second appear to be completely analogous as far as implementation and performance are concerned. Both require the same aperture sizes to get the required resolution and both suffer from the same aberration problems associated with using a standard low F/D parabolic reflector which is not focused at infinity. Both methods also require the use of sidelobe

suppression techniques. The only advantages occur when a larger F/D reflector is used. For F/D numbers of the order of unity or more, it is possible to fix both the transmitter and receiver and scan only the reflector. This method is appealing because of its simplicity of implementation, but it suffers from severe off-axis aberrations for F/D < 1 and angles of view greater than 10^{o}. Because standard parabolic reflectors come with F/D values between 0.25 and 0.4, it would require a large tooling charge to implement this scheme.

The third method listed has the advantage of very low sidelobes. Since both the transmit and receive antenna sidelobes are superimposed on the target, the net result is that the depth of the sidelobes is doubled in decibels. This is a tremendous advantage where enhanced image dynamic range is a requirement.

The fourth method listed above has the advantage of a precisely determined resolution spot size with virtually no sidelobes, but it has the disadvantage of a large area return signal from the absorptive panel which is a potential range quietness problem. Focusing the transmitter and/or receiver antennas on the hole would help, but it would require moving the target through a raster scan behind the hole which could be difficult in the case of a large target.

D. Direct Versus Indirect Imaging Techniques

It was decided for this program that a direct angle-angle approach using a pair of standard parabolic antennas represents the most practical method of rapidly obtaining millimeter wave imaging results. The advantages of using this direct imaging method are:

1. Very large image dynamic range (> 40 dB).
2. Faster results. Images can be viewed as they are scanned out.
3. Less complex receivers. Phase measurements are not required.
4. The type of mechanical scanning required is easier to implement.

5. Open test range may be used (-30 dBsm expected).

The main disadvantages are the image aberration caused by focusing the parabolas at a finite range, and caused by a limited depth of field at focus. These problems have been analyzed theoretically for our current system design, and though there is some deterioration of resolution, it does not appear to be of a serious nature.

The apodization required to reduce the sidelobe levels is not expected to be a problem. The results obtained in practice give confidence that the two-way sidelobes of the dual transmit and receive antennas will easily reach -40 dB; i.e., 40 dB image dynamic range.

It is recognized that there are differences in the millimeter wave images produced by the range-angle and the angle-angle imaging techniques. It is believed, however, that the number of scattering centers in an angle-angle image, their location with respect to the target geometry, and their relative intensity as a function of target composition will provide a valuable set of data for projecting the effectiveness of a range-doppler imaging system. The simplicity with which the angle-angle scanning technique can be implemented was an important factor in choosing this approach for this program.

III. TECHNICAL DETAILS

A. General Design of Imaging Experiment

Figure 1 is a schematic diagram of the dual transmit and receive antennas now being implemented to produce scanned angle-angle images of targets at 3.2 mm wavelength. The parabolic dishes have F/D = 0.333 and are focused at a range of 48 ft. The basic equation determining the antenna diameter D for a required target resolution length δ_T at range R is given in the coherent imaging case by the Sparrow Criteria[2]

$$\frac{\delta_T}{R} = \frac{1.464\,\lambda}{D} \tag{1}$$

where λ is the wavelength. This resolution limit is about 20% larger than the noncoherent Rayleigh criteria.

Image dynamic range in direct imaging processes must be defined in terms of the sidelobes which arise as a result of the use of a finite aperture. The well known Airy's intensity distribution function for the image of a point source generated with a lens of aperture diameter D is given by

$$I = I_o \left[\frac{2J_1\left(\frac{\pi D \rho}{\lambda F}\right)}{\left(\frac{\pi D \rho}{\lambda F}\right)} \right]^2 \tag{2}$$

where $J_1(x)$ is the first order Bessel Function, ρ is the radius in the image plane, and F is the focal length. Figure 2 shows a plot of I^2 over the first five rings (far-field case). The first ring intensity level essentially determines the dynamic range allowable between two point sources which are separated by one resolution length. If the radiated power of the second source has the same intensity as the first ring of the stronger source, the central lobe of the lower power source may be entirely masked out, depending upon the phase relationships.

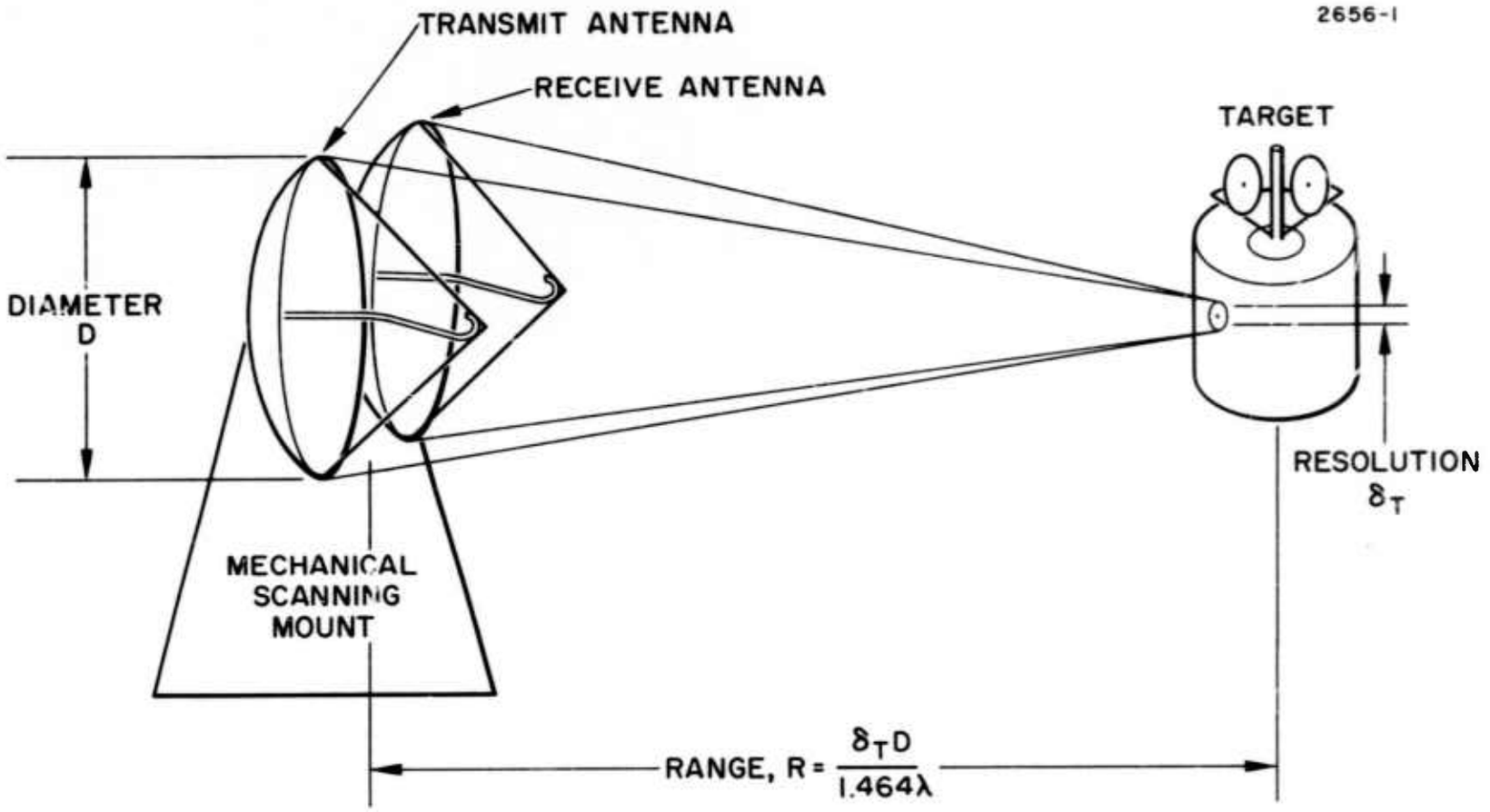

Fig. 1. Physical arrangement for mechanically scanned millimeter wave images.

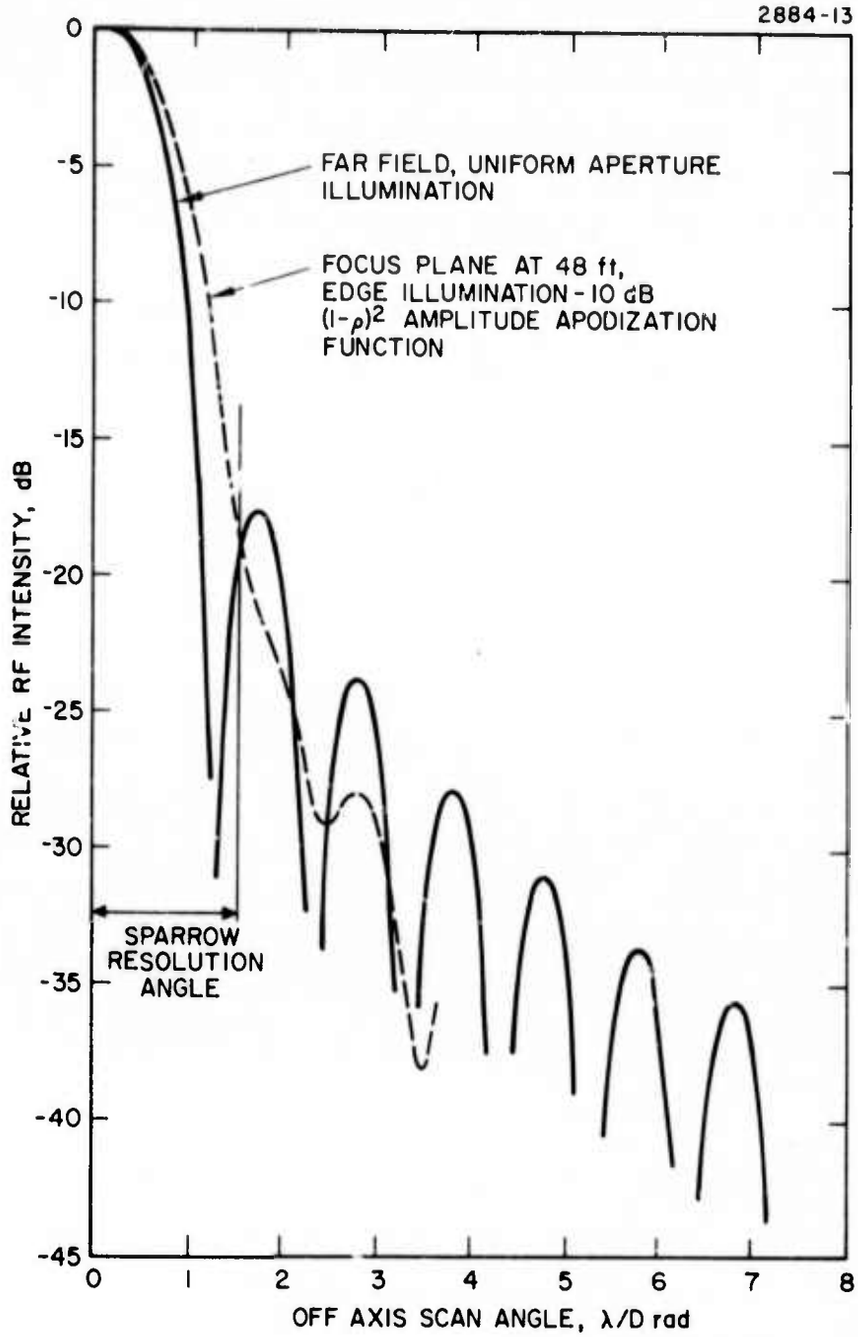

Fig. 2. Target transmit/receive pattern for a single point scatterer. Calculated using two parabolic dishes with F/D = 0.333.

By the same arguments, sources separated by several resolution lengths would be allowed a much greater dynamic range. Figure 2 shows that for dual scanning antennas the allowable dynamic range between two point scatterers separated by one resolution length is ~35 dB. By apodization techniques it is possible to further reduce the level of the sidelobes at the expense of slightly widening the central lobe. This is usually accomplished by diminishing the amplitude of the received signals as a function of reflector radius.[3] A standard technique is to use a feed horn which has a beamwidth narrower than the angle subtended by the reflector.

The image dynamic range obtainable with the current system has been analyzed by a computer analysis of the Fourier transform for a parabolic reflector with an amplitude illumination varying as $(1 - \rho^2)$ (ρ is the aperture radius variable). The illumination was assumed to be down 10 dB at the edges of the reflector. The results are plotted in Fig. 2 along with the nonapodized far-field case. Note that the amplitude falls off to only -38 dB at the Sparrow resolution angle for which the system was designed, but that it goes well below -40 dB with only a 10% degradation in resolution and is below -55 dB at 1.5 times the resolution angle. When the point scatterer is moved ±3 ft out of the focal plane, the resulting pattern is deteriorated at most by 1.5 dB. It is thus believed that excellent image dynamic range will be achievable with this system.

B. Analysis of Parabolic Antenna Receiver Response

Figure 3 shows the model that was used to analyze the receiver response for a parabolic antenna focused on a point source and then allowed to scan in angle ϕ. This model includes the effect of aberrations caused by focusing the parabola in its rear field but it neglects all polarization effects.

The analysis proceeds by letting each differential element in the aperture, $r_a dr_a d\theta$, be a reflector of the source energy falling upon it and then integrating over the aperture to obtain the total energy

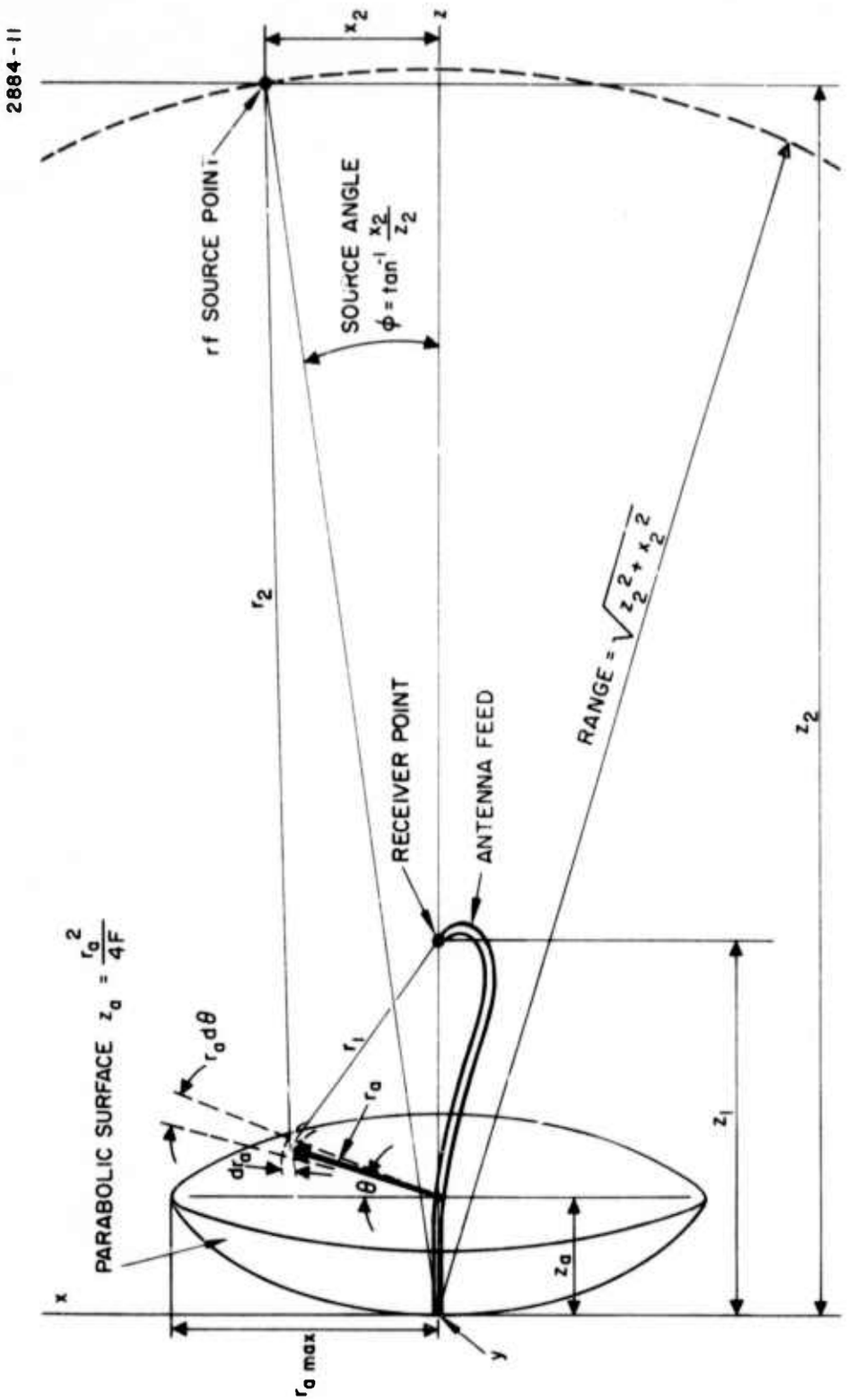

Fig. 3. Model used to analyze receiver antenna response.

arriving at the receiver. The rf field arriving at the aperture element located at (r_a, θ, z_a) varies in phase and amplitude as a spherical wave emanating from the point source at $(x_2, 0, z_2)$. Therefore, we may write[2]

$$\text{Differential aperture field} \sim \frac{e^{-jkr_2}}{r_2}$$

where

$$k = 2\pi/\lambda$$

and

$$r_2 = \sqrt{x_2^2 + r_a^2 + (z_2 - z_a)^2 - 2x_2 r_a \cos\theta} \qquad (3)$$

is the distance from the source point to the aperture element. Similarly, we may now treat the aperture element as a point source from which a spherical wave front proceeds to the receiver at point $(0, 0, z_1)$

$$\text{Differential receiver field} \sim \frac{e^{-jkr_2}}{r_2} \cdot \frac{e^{-jkr_1}}{r_1}$$

where

$$r_1 = \sqrt{r_a^2 + (z_1 - z_a)^2} \qquad (4)$$

is the distance from the aperture element to the receiver point. An additional amplitude factor may be included in the differential receiver field to account for the field pattern of the antenna feed at the receiver point. In this study we have assumed that this amplitude factor takes the form

$$A = 1 - (C_1 r_a)^2 \qquad (5)$$

where C_1 is a constant determined by the fraction of the rf energy received from the edge of the antenna (often called the "edge illumination"). For example, for a feed horn pattern which drops off to -10 dB power at the edge of the antenna, C_1 is determined by the boundary condition to be

$$C_1 = \sqrt{1 - 0.316}/r_{a\,max} \tag{6}$$

and A varies between 1 and 0.316 ($1 \leq A^2 \leq 0.1$).

The value of the received signal for a fixed source point is given by summing the contributions from all differential elements in the aperture at the receiver point. Thus

$$\text{Received signal} \propto \psi = \int_0^{r_{a\,max}} \int_0^{2\pi} A \frac{e^{-jk(r_2+r_1)}}{r_1 r_2} r_a dr_a d\theta \tag{7}$$

where r_2, r_1, and A are given in eq. (3) through (6), respectively.

For the purpose of digital computation the integrals in eq. (4) were evaluated using Simpson's Rule[4] as an approximation to the integrals. The angular integration was broken up into eight steps for each half-wavelength change in path length from the source, and the number of radial integration steps was set equal to four times the Fresnel number of the aperture. These step sizes were found to give adequate accuracy in both phase and amplitude. The relative receiver power was calculated from the function ψ as Receiver power $\propto \psi_r^2 + \psi_i^2$ where ψ_r and ψ_i are the real and imaginary parts of ψ given by

$$\begin{bmatrix} \psi_r \\ \psi_i \end{bmatrix} = \int_0^{r_{a\,max}} \int_0^{2\pi} \frac{A}{r_1 r_2} \begin{bmatrix} \cos k(r_2 + r_1) \\ -\sin k(r_2 + r_1) \end{bmatrix} r_a dr_a d\theta \quad .$$

The relative receiver phase was calculated from

$$\text{Receiver phase} = \tan^{-1}\left(\frac{\psi_i}{\psi_r}\right) \quad .$$

In Figs. 4 through 6 the relative rf power and the phase are plotted for some cases of interest using a parabolic reflector of the desired diameter and a range of 48 ft (14.6 m). This range was calculated from the Sparrow resolution criteria given in eq. (1).

Figure 4 shows the parabolic aberration which occurs as a result of focusing the antenna in the near field at a range of 48 ft. These calculations were performed for uniform aperture illumination in order to show the effects clearly. Note that considerable distortion occurs for the case of F/D = 0.333 but that the actual sidelobe degradation is still fairly small.

Figure 5 shows the added effects of apodization when F/D is held at the value of 0.333 and the focus point at 48 ft. The apodization factor was assumed to vary as in eq. (5). Note that the central lobe is widened somewhat and that the sidelobe levels are decreased.

Figure 5(c) shows the final expected image of a point source which is in focus. The two focus points were calculated from the thin lens formula

$$\frac{1}{F} = \frac{1}{z_1} + \frac{1}{z_2} \quad .$$

Figure 6 shows the degradation of the imaged spot when the point source is moved in 3 ft intervals on either side of the focal plane. These calculations show that the spot widths and sidelobe degradation is less than 1.5 dB for a depth of field of ±3 ft.

It is concluded from this study that a standard F/D = 0.333, parabolic antenna will give satisfactory performance in this application even though there are considerable aberration effects. Degradation of the spot size from the desired performance is expected to be 10% at most due to parabolic aberration because most of the central spot broadening is caused by the required apodization.

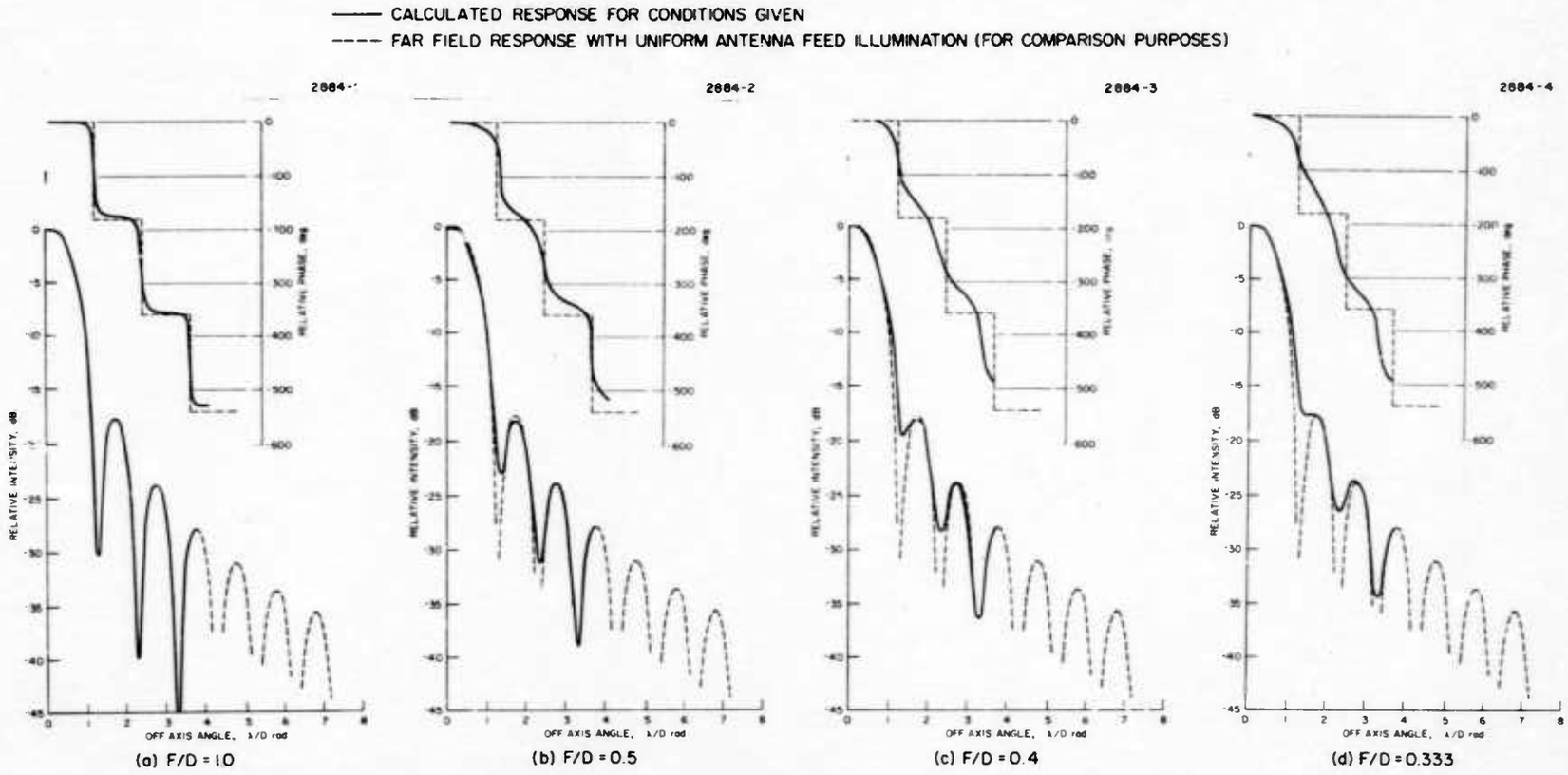

Fig. 4. Calculated rf response for a parabolic antenna focused at a point source 48 ft down range and scanned in angle. (Uniform aperture illumination is assumed and the antenna focal lengths were calculated from the thin lens formula $1/F = 1/z_1 + 1/z_2$).

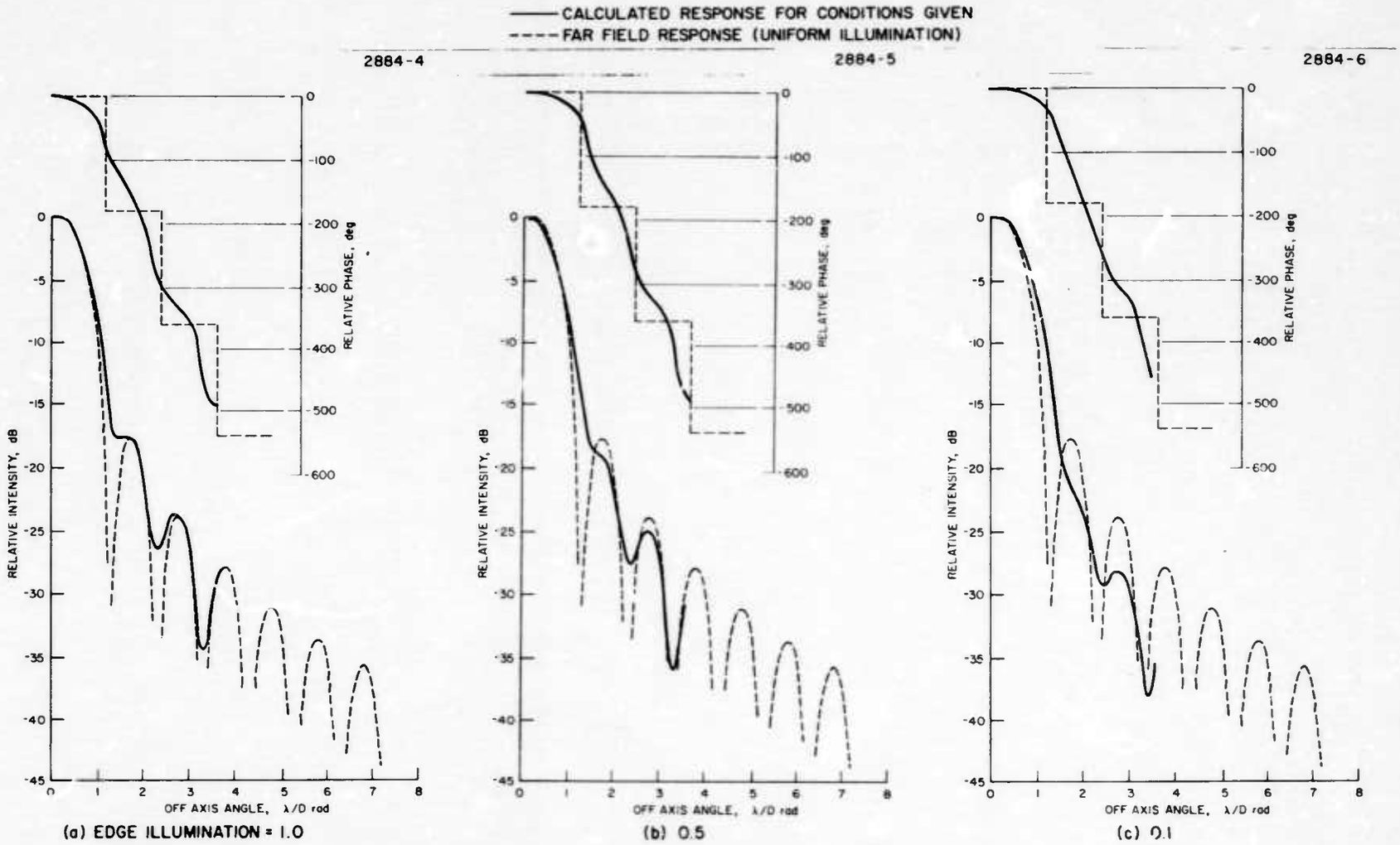

Fig. 5. Calculated rf response for a parabolic antenna of diameter D focused at a point source 48 ft down range and scanned in angle. (F/D = 0.333 and focal points held constant).

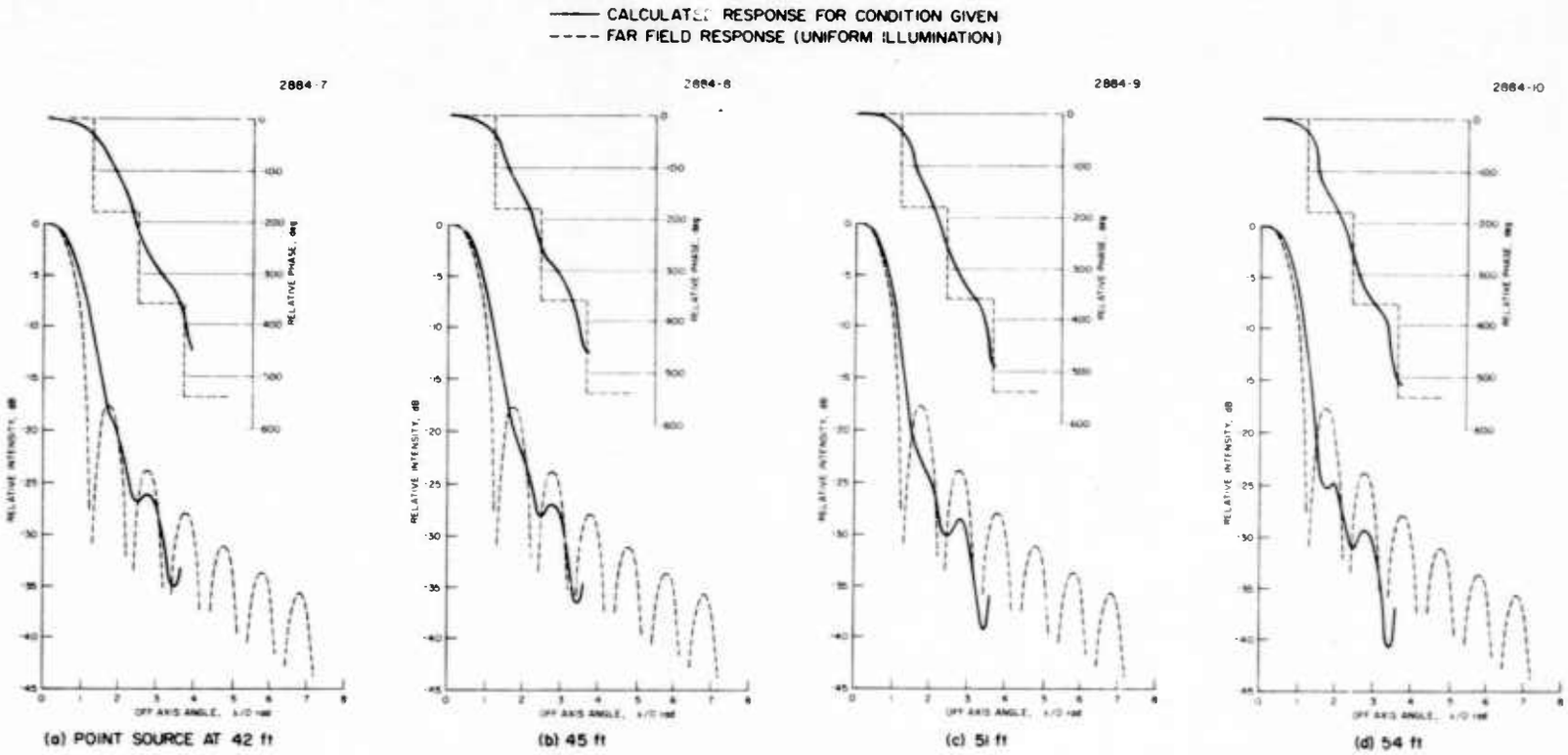

Fig. 6. Calculated rf response for a parabolic antenna focused at 48 ft and scanned in angle. (F/D = 0.333, edge illumination = 0.1, focal points held constant).

C. Test Range Design

A primary consideration for our current imaging program has been test range quietness. We have chosen to solve this problem by using an outdoor range where the targets are suspended above the horizon so that very little range backscatter can occur. Figures 7 through 10 show schematically and photographically, the position of the test range which achieves this result. Our goal for this system is a threshold of -30 dBsm which we believe is achievable with this range and with the aid of some interantenna leakage suppression techniques.

The target suspension system consists of two 30 ft steel poles separated by 50 ft (55^{o} horizontal angle of view) and placed at the top of a hill facing the ocean. The vertical angle of view for a target suspended at 20 ft height is 7^{o} above the horizon, and for 18^{o} below the horizon there are no obstructions for 1000 ft. Since the 40 dB beamwidth of the transceiver is much smaller than the angle of view, this range configuration is expected to give excellent results.

D. 94 GHz Receiver

Figure 11 is a diagram of the transmitter-receiver system as it is now configured. The 94 GHz rf source is a Hughes LOW-1 backward wave oscillator (BWO) which has greater than 1 W available power. This BWO is frequency locked to the klystron local oscillator in order to provide a stable 30 MHz i.f. frequency. The mixers used in this receiver were fabricated at Hughes Research Laboratories. They are 2 μm dot-size Schottky barrier diodes which have about 7 to 8 dB conversion loss and a noise figure less than 10 dB. The i.f. amplifiers have a tangential sensitivity of about -100 dBm and a bandwidth of 10 MHz, thus giving the overall receiver a sensitivity of about -92 dBm.

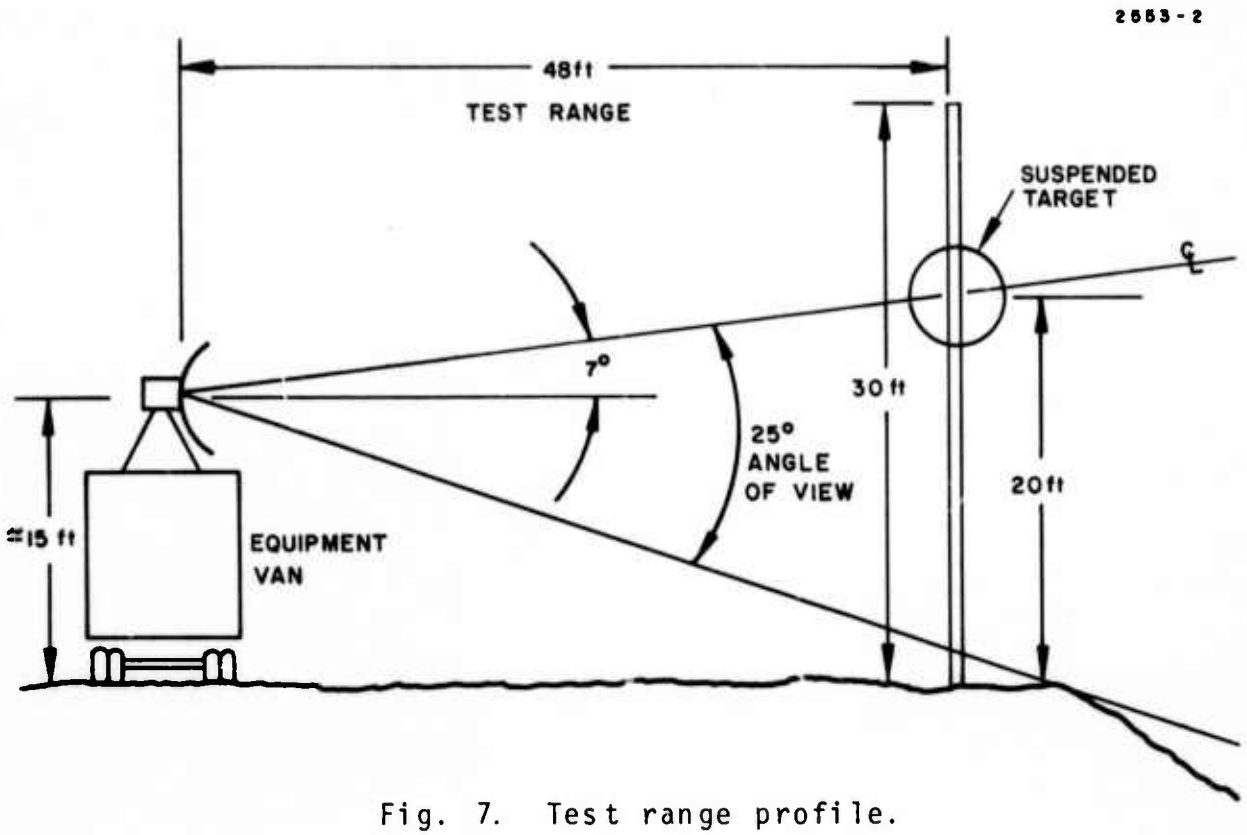

Fig. 7. Test range profile.

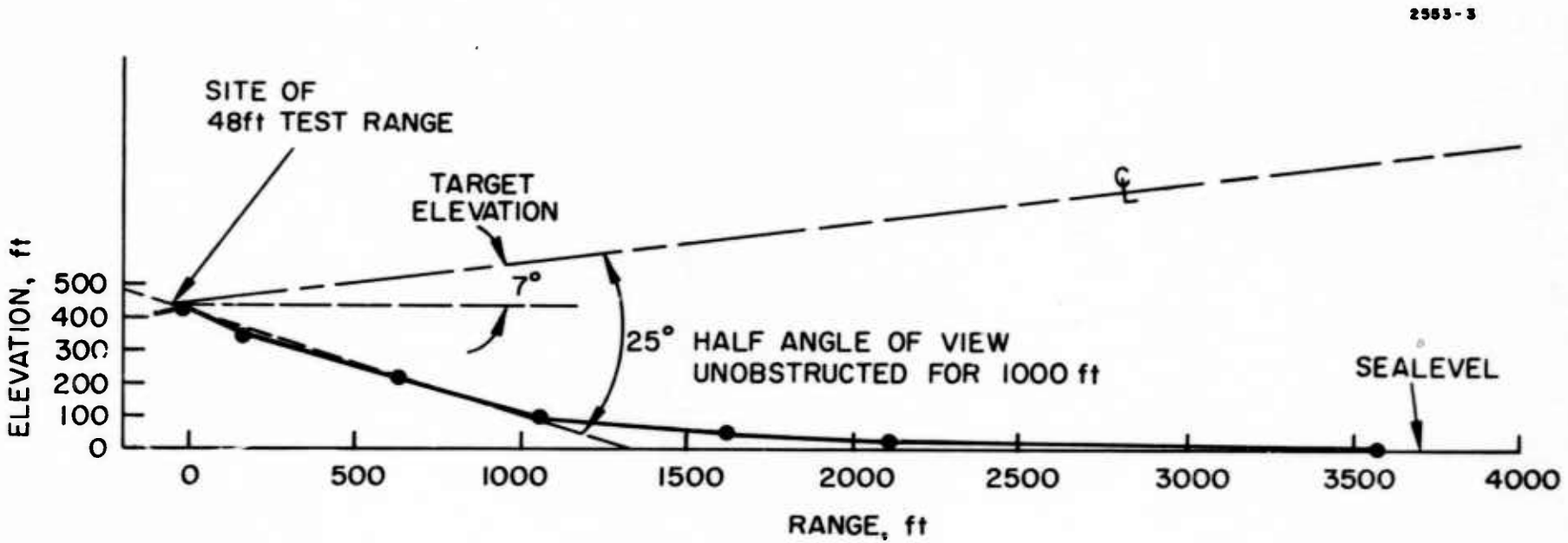

Fig. 8. Terrain elevation versus range (facing south).

M10035

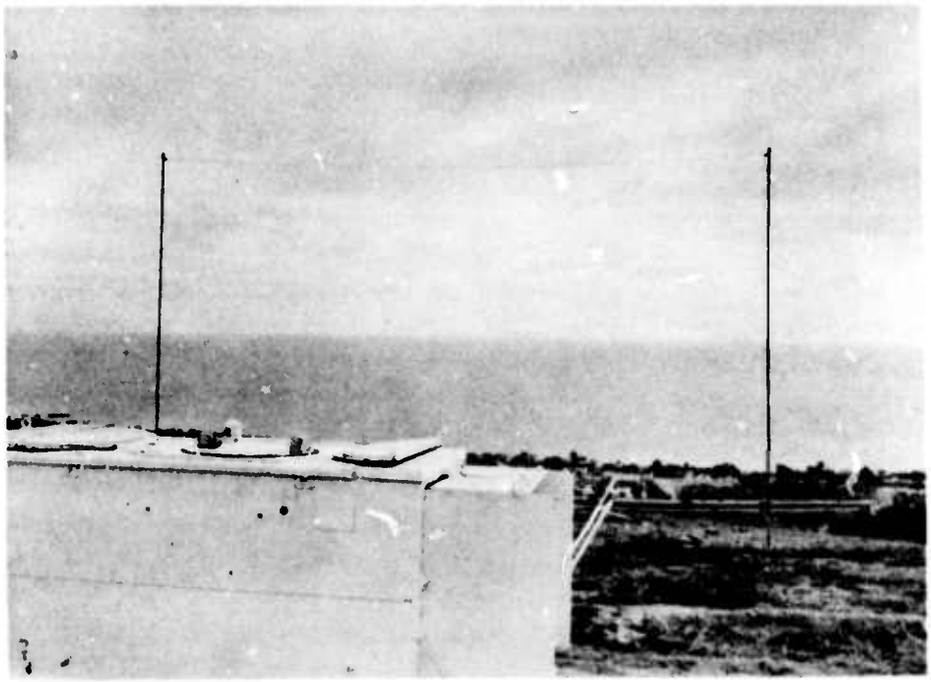

Fig. 9. Facing south from test range.

M10034

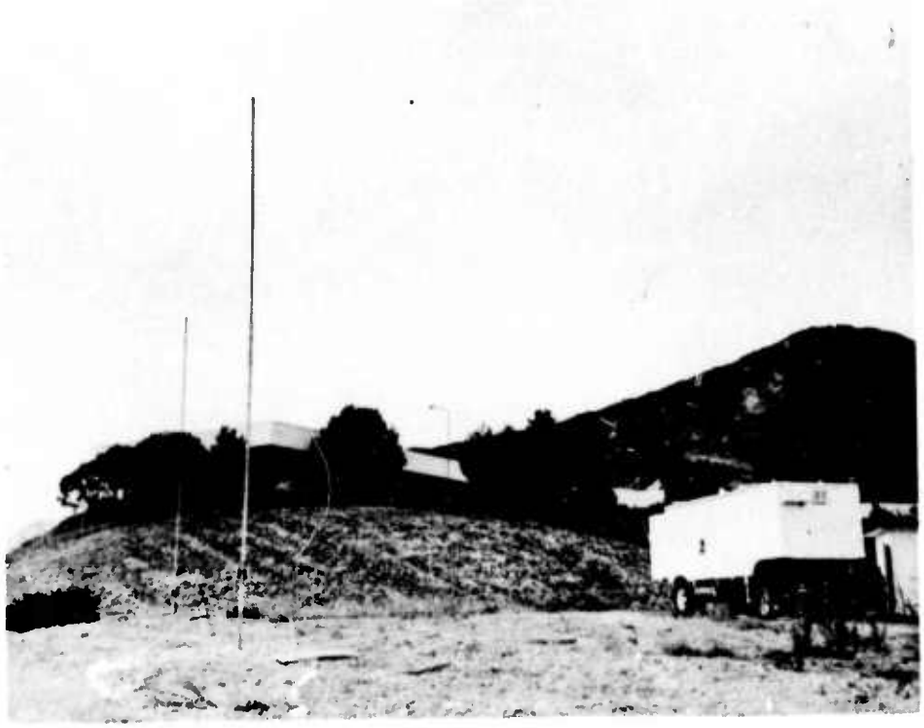

Fig. 10. Facing across range toward HRL.

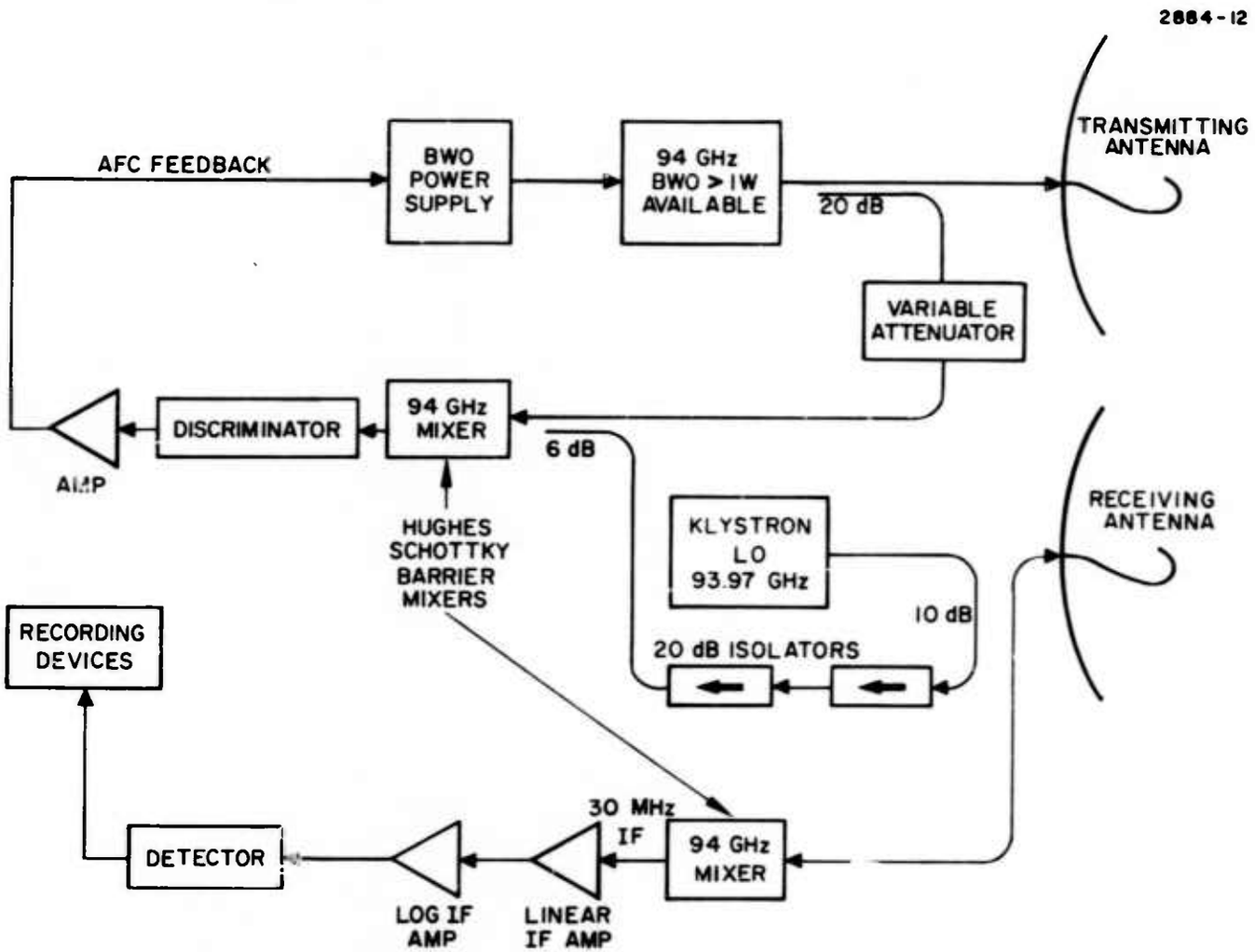

Fig. 11. Millimeter wave transmitter and receiver.

IV. TEST PROGRAM

Under the current program we have proposed to accomplish the following two tasks.

1. The range installation as described in Section III-C will be completed, aligned, and calibrated. This is anticipated to be essentially completed by the end of November 1973 under the current contract.

2. A small set of elemental, composite, and integral structures will be scanned both to establish the first order image properties and to assess the performance limits achieved by the system.

The range is presently complete except for the mounting of the rf transmitter, receiver, and scanning pedestal in the equipment trailer. All of this equipment has been tested in the laboratory and is functioning well. The receiver has -90 dBm threshold sensitivity which is far greater than required. A log i.f. amplifier yields better than 50 dB dynamic range.

Because of changes in the program, the antennas were not ordered until September and will not be delivered until December 1973. These antennas will be focused and tested by the manufacturer to assure minimum spot size at the desired range and, therefore, will be ready to use as soon as they arrive.

The imaging system will be calibrated by imaging a single polished sphere. The resulting images will show spot size and symmetry and the various sidelobe levels. The theoretical cross section of the sphere will be used to determine the relative target scattering cross sections for all targets.

The test program will include multiple views of approximately ten different targets. These targets will include typical single scatterers such as the following:

1. Sphere 4.5 in. diameter (-20 dBsm)

2. Cylinder (2 to 5 cm diameter)

3. Dihedral and trihedral corners (~2 to 5 cm across)

4. Metal and dielectric flat surfaces (2 to 5 cm diameter)

5. Metal surfaces with different degrees of roughness

6. A section of an actual solar panel

7. A piece of thermal blanket material used on communication satellites.

In addition to these targets, more complex structures made up of multiple elementary scatterers will be imaged. This test procedure should provide a good basis for evaluating both the imaging system and the effectiveness of millimeter wave images for identifying target geometry.

V. SUMMARY

Many delays and changes of plan have been encountered in this program, but we still feel that it will be possible to get some first order millimeter wave imaging results before the end of 1973. To take full advantage of the potential of the program, however, a proposal has been submitted to ARPA for a continuation of the measurements into 1974. Of particular interest is the opportunity to make measurements on the qualification model of the Lincoln Laboratories LES-6 satellite which is now available. This model has already been imaged at X band and at 10.6 μm which will provide interesting comparisons.

The test range and all associated equipment are nearly complete except for the parabolic antennas which are scheduled for delivery in December. All of the components have been tested in the laboratory and found to be functioning satisfactorily. As soon as the antennas arrive they can be bolted in place and the test phase of the program can be completed.

REFERENCES

1. G. N. Ramachandran and A. V. Lakshminarayanan, Proc. Nat. Acad. Sci., Vol 68, p. 2236, September 1971.

2. G. B. Parrat and B. J. Thompson, Physical Optics Notebook, Society of Photo-Optical Instrumentation Engineers, Redondo Beach, California, (1969) p. 2.

3. John W. Sherman, III, "Aperture-Antenna Analysis," Chapter 9 of Radar Handbook, M. I. Skolnik, Editor, McGraw-Hill, 1970, pp. 9-21.

4. H. B. Dwight, Tables of Integrals and Other Mathematical Data, (The McMillan Co., N. Y., 1961) p. 250.